Case Study: Model Test on the Effects of Grade Control Datum Drop on the Upstream Bed Morphology in Shiting River

Xudong Ma, Lu Wang *, Ruihua Nie, Kejun Yang and Xingnian Liu

State Key Laboratory of Hydraulics & Mountain River Engineering, Sichuan University, Chengdu 610065, China; maxd@scu.edu.cn (X.M.); nierh@scu.edu.cn (R.N.); yangkejun@scu.edu.cn (K.Y.); liuxingnian@126.com (X.L.)

* Correspondence: wanglu@scu.edu.cn

Abstract: This paper conducted an undistorted scaled model test (geometric scale λ_L = 1:80; the others are derived scales based on Froude similitude) of a 1.3 km-long river reach in Shiting River, China, investigating the impacts of the grade control datum (GCD, defined as the crest elevation of the grade control structure) drop on the upstream bed morphology. Three GCDs and six flood events (occurrence probability 1–50%, discharge = 600–4039 m^3/s) were tested on the model. Experimental results indicate that, for a constant GCD, the increase in discharge deepens and widens the upstream river bed. For a lower GCD, the increase in channel depth and width caused by the increasing discharge is greater. For each discharge, the decrease in GCD induces a lower and steeper upstream river bed, widening the upstream main channel. For lower discharge, the GCD drop induces a head cut erosion area upstream of the grade control structure and the head cut erosion area is filled by the upstream sediment when the flow discharge is high. Experimental data also indicate that the maximum general scour depth at the 105th Provincial Highway Bridge is approximately independent of discharge for a constant GCD. For a lower GCD, the general scour depth at the 105th Provincial Highway Bridge increases slightly with discharge.

Keywords: bed morphology; bridge scour; general scour; grade control

1. Introduction

Scour is a main design concern for hydraulic structures such as bridge or wind turbine foundations [1–4], buried pipelines [5–7], weirs and sills [8–12], etc. The scour at instream structures can be classified into three types: general scour, constriction scour and local scour [13–15]. The general scour is normally caused by the evolution of the river bed and is independent of the instream structure. The constriction scour occurs where an instream structure narrows the flow section. The local scour is caused directly by the change of flow pattern induced by the existence of the instream structure.

Bed degradation usually occurs when the bed erosion rate is greater than the upstream sediment replenishment rate. It can induce general scour at the foundations of instream structures and destabilize riverbanks, threatening the security of both the public and private properties [16]. Grade control structures (GCSs) such as submerged weirs, bed sills and check dams are common countermeasures for bed degradation [9–11,17–19]. They can raise the upstream water level and reduce the flow capacity for sediment transport, preventing the upstream river bed from being excessively degraded. Properly designed GCSs play a role as a grade control datum (GCD) for the upstream river reach [16,20]. The GCD is usually the crest elevation of the GCS which is lower than the upstream bed level.

However, the flow over GCSs can cause local scour [8–12], and the downstream general scour may continue if there are no further downstream GCSs, leading to structural damages or failures

(Figure 1). The failure of a GCS induces a drop in GCD, accelerating the adverse impacts they are initially built to prevent [16]. Thus, it is important to understand the scour process at GCDs for safe design. Also, understanding the impacts of GCD drop on the upstream bed morphology can help to assess the stability of the upstream riverbanks and instream structures if the GCS fails.

Figure 1. Scour at the grade control structure (GCS) downstream of the 105th Provincial Highway Bridge after the flood event on 9 July 2013 (discharge $Q = 2710$ m^3/s).

The local scours at GCSs have been extensively studied and many empirical equations have been proposed [8,10–12,21–38]. Some studies also investigated the impacts of GCSs on the river bed profile [17,18]. Although very important, no studies have investigated the effects of GCS failure (i.e., GCD drop) on the upstream river reach. This paper conducted a scaled model test based on a 1.3 km-long river reach upstream of a GCS in Shiting River, China, investigating the effects of GCD drop on the upstream riverbed morphology.

2. Background

Shiting River is the first tributary of Tuo River. It originates from the Longmen mountain located in Sichuan Province, China, having a length of 131.7 km and a basin area of 1501 km^2. The mountainous reach (upstream reach) of the Shiting River is 61.1 km long with a gradient between 92.3–10.4‰. The gradient of the river reach downstream of the mountain decreases gradually and ranges between 12 and 2.5‰ before it joins the Tuo River. Since the Wenchuan Earthquake (Ms 8.0) in 2008, serious bed degradation occurred in the piedmont reach of Shiting River, significantly exposing and endangering the foundations of instream infrastructures [39,40]. Thus, grade control structures (GCSs) were extensively used in this river reach as countermeasures for bed degradation.

The studied reach is about 13 km downstream of the mountainous area with a gradient of around 4‰, in which the 105th Provincial Highway Bridge is located (Figure 2). The studied reach is about 1.3 km upstream of the 105th Provincial Highway bridge, and has a channel width between 300–400 m. This reach is a quasi-straight channel and has no instream structures upstream of the 105th Provincial Highway Bridge. Thus, the impacts of stream curve and other instream structures on the bed morphology are negligible. As mentioned previously, significant bed degradation occurred in the piedmont reach of Shiting River after 2008 [39,40]. Thus, an 18 m high grade control structure was built upstream of the studied reach (2 km upstream of the 105th Provincial Highway Bridge) for stabilizing the upstream riverbed. The flood events during the period of 2009–2012 degraded the river bed at the 105th provincial Hyghway Bridge to an elevation of 539 m (544 m before the Wenchuan Earthquake). In 2012, for protecting the upstream river reach and the bridge, a grade control

structure (GCS) with a downstream stilling basin (for minimizing the downstream local scour) was built downstream of the 105th Provincial Highway Bridge with a crest at $z = 539$ m (i.e., grade control datum, GCD). However, as the bed degradation downstream of the GCS continued after the flood event in July 2013 ($Q = 2710$ m³/s), the bed elevation downstream of the GCS became 527 m, exposing the GCS foundation and causing structural failure (Figure 1). In order to assess the impacts of GCD drop (or GCS failure) on the upstream bed morphology, as well as the general scour depth at the 105th Provincial Highway Bridge, a scaled model test is conducted in this study.

Figure 2. Plan view of the studied reach of Shiting River (**a**); location of Shiting River (**b**); a photo of the model (**c**).

3. Experimental Setup

An undistorted model based on the prototype shown in Figure 2 was built with a geometry scale $\lambda_L = 1:80$ in the State Key Laboratory of Hydraulics and Mountain River Engineering, Sichuan University, China. The scaled model was implemented into a water-recirculating system. The bank revetments were built in concrete and had a 0.5 m-deep non-cohesive sediment bed. The flow passed through a triangular weir for flowrate measurement before entering the model, and exited the model through the concrete grade control datum as a free flow which is the same as that of the prototype.

Froude similitude [41] was adopted for the flow motion. Thus, the velocity scale is $\lambda_U = \lambda_L^{0.5} = 8.94$, the discharge scale is $\lambda_Q = \lambda_L^{2.5} = 1{:}57243$ and the time scale is $\lambda_t = \lambda_L^{0.5} = 8.94$. In order to achieve the similitude of sediment motion, U/U_c in the prototype and model should be the same (U_c is the critical velocity of the sediment entrainment). The Shamov formula (Equation (1)) is commonly used for calculating U_c in a scale model test, as it is simple to use and can provide reliable estimations [42].

$$\frac{U_c}{\sqrt{gd}} = 1.47\left(\frac{h}{d}\right)^{1/6} \tag{1}$$

where g is gravity acceleration, h is approach flow depth, d is sediment size. Based on Equation (1), the sediment size scale is $\lambda_d = \lambda^2{}_{Uc} = \lambda^2{}_U = 1{:}80$. The model sediment was scaled down by $\lambda_d = 1{:}80$ from the prototype sediment size distribution based on a field survey in the studied river reach (Figure 3). As there is an 18 m-high grade control structure with a stilling basin (for minimizing the downstream local scour) located about 2 km upstream of the 105th Provincial Highway Bridge, the upstream sediment is blocked by the grade control structure from entering the studied river reach. Therefore, the upstream sediment replenish rate was considered as zero and no sediment was fed during the test.
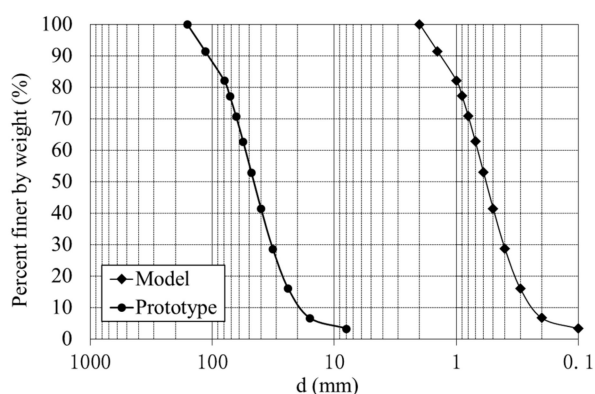

Figure 3. Grain size distribution of the prototype and model sediment.

Six flood events (discharge Q = 600–4039 m³/s, occurrence probability P = 1%–50%) were tested for three GCDs (z = 527 m, 533 m, 539 m). Among which, z = 539 m is the crest of the current GCS, z = 533 m is the crest elevation of the new GCS design plan, z = 527 m is the bed level downstream of the GCS after the flood event on 9 July 2013.

The tests of each z commenced with an initially flattened sediment bed and the smallest discharge Q. The gradient of the initial flat bed was set at 4‰, which is the average bed gradient of the studied reach after the flood event in July, 2013. The test stopped and the water dried gradually after the scaled flood duration t. Then, the bed profile was measured using a Total Station (Nikon, Japan, DTM-352C). The next test, with a higher discharge, commenced without flattening of the sediment bed.

Before the formal tests, a preliminary test based on the flood event on 9 July 2013 (Q = 2710 m³/s) was conducted for model calibration. As this model test is aimed to assess the impacts of GCD drop on the upstream bed morphology, only the bed profile upstream of the GCS was measured for calibration. Based on a field survey after the flood event on July 9 2013, the average gradient of the studied river reach was 4‰. The measured model talweg profile of the calibration test has an average gradient of 4.3‰ (multiple correlation coefficient R^2 = 0.91), which is close to that of the prototype. The discrepancy of bed profile between the model and prototype is within ± 0.8 m (prototype vaule), which is acceptable for the large scale prototype of this study. As the scour design for instream structures normally adds a safe value greater than 1 m to the estimated scour depth, the model data is reliable for engineering use.

4. Results and Discussions

The experimental results and conditions are summarized in Table 1. In Table 1, P is the probability of a flood event; Q is the prototype flood event discharge; t is the prototype flood event duration; z is the prototype grade control datum elevation; i is the measured average bed slope (model) upstream of the GCS; d_p is the maximum general scour depth at the site of 105th Provincial Highway Bridge in terms of $z = 544$ m (i.e., the bed elevation before the Wenchuan Earthquake). In this study, as the detailed hydrograph is not available, the peak flood rate was applied during each flood event. As the flood in this area is caused by intense rain, the flood rising and recession periods are very short and can be neglected. In order to avoid the impacts of local scour and constriction scour on the bed profile, the general scour depth at bridge site was measured upstream of the scour area of the bridge foundation.

Table 1. Summary of the experimental conditions and results.

Group	P	Q	z	i	d_p	t
Number	(%)	(m^3/s)	(m)	(‰)	(m)	(h)
1	50	600	539	4.5	4.9	54
2	20	1225	539	4.4	5.2	36
3	10	2095	539	4.3	5.3	36
4	5	2664	539	4.3	5.3	36
5	3.3	2935	539	3.8	5.5	24
6	1	4039	539	3.8	5.7	24
7	50	600	533	8.5	9.4	54
8	20	1225	533	7.7	9.9	36
9	10	2095	533	6.3	10.2	36
10	5	2664	533	5.5	10.6	36
11	3.3	2935	533	5.3	10.7	24
12	1	4039	533	4.9	10.9	24
13	50	600	527	12.6	14.8	54
14	20	1225	527	10.2	15.5	36
15	10	2095	527	8.2	16	36
16	5	2664	527	7.2	16.5	36
17	3.3	2935	527	6.2	17.2	24
18	1	4039	527	4.9	17.6	24

4.1. Talweg Profile Upstream of GCS

Figure 4 shows the talweg profile upstream of the GCS of each GCD z for different flood events. Figure 4 indicates that, for each test, the bed elevation immediately upstream of the GCS is approximately equal to the GCS crest (i.e., GCD). For each z, the upstream talweg elevation is lower with a lower P (higher discharge, Q). This is because a higher flowrate has a greater capacity for sediment transport, causing more erosion on the bed. For $z = 539$ m, the bed in -150 m $< x < 0$ is flatter with a higher Q, as some of the sediment driven by the approach flow is blocked by the GCS, resulting in an aggraded bed near the GCS. For $z = 533$ m and $z = 527$ m, the aggradation in -150 m $< x < 0$ disappears. This is because, for a lower GCD, the sediment above the GCD is flushed downstream over the GCS without any blockage. Figure 4 also indicates that, for a lower z, the difference in the talweg profile caused by increasing Q is larger. The bed incision due to GCD drop can be affected by two factors: (i) the approach flow capacity for sediment transport; (ii) GCS blockage. The bed is stabilized when these two factors reach a balance. As the GCS only blocks the sediment when the GCD is above the bed, for a lower GCD, factors (i) and (ii) reach the balance at a lower bed level.
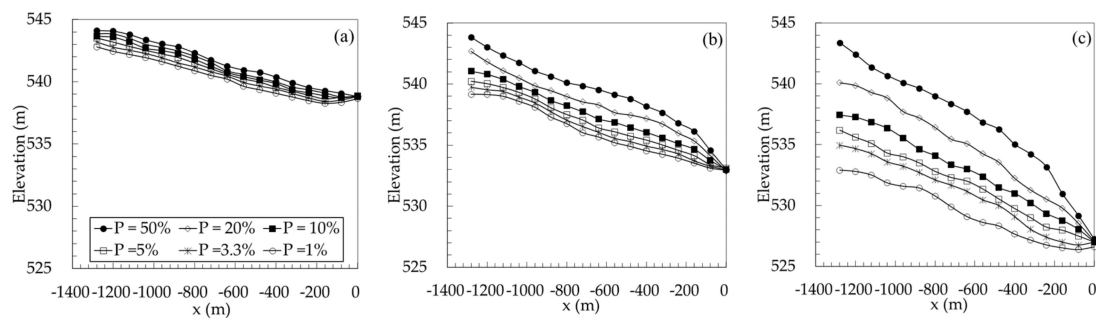
Figure 4. Upstream talweg profile after different flood events for $z = 539$ m (**a**), $z = 533$ m (**b**) and $z = 527$ m (**c**).

Figure 5 indicates that for each Q, the upstream talweg elevation decreases with decreasing z. For $P = 50\%$, there is an abrupt steepening in the talweg profile for $z = 533$ m and 527 m at $x \approx 200$ m and $x \approx 300$ m, respectively. For $P \leq 10\%$, the abrupt steepening in the talweg profile for $z = 533$ m and 527 m disappears. This is because the bed degradation induced by the drop in GCD begins as a head cut erosion process from $x = 0$. For small discharges ($P \geq 20\%$), the sediment transport rate is slow and is unable to fill the head cut erosion area during the flood event. For high discharges ($P \leq 10\%$), the upstream sediment transport rate is high enough to fill the head cut erosion area within the duration of the flood. Figure 5 also indicates that for $P \leq 3.3\%$, the talweg profile of -200 m $< x < 0$ is flatter than that of $x < -200$ m for $z = 527$ m. This is because the grade control datum protrudes high enough above the upstream river bed to block the sediment from the upstream, inducing an aggraded bed near the GCS.
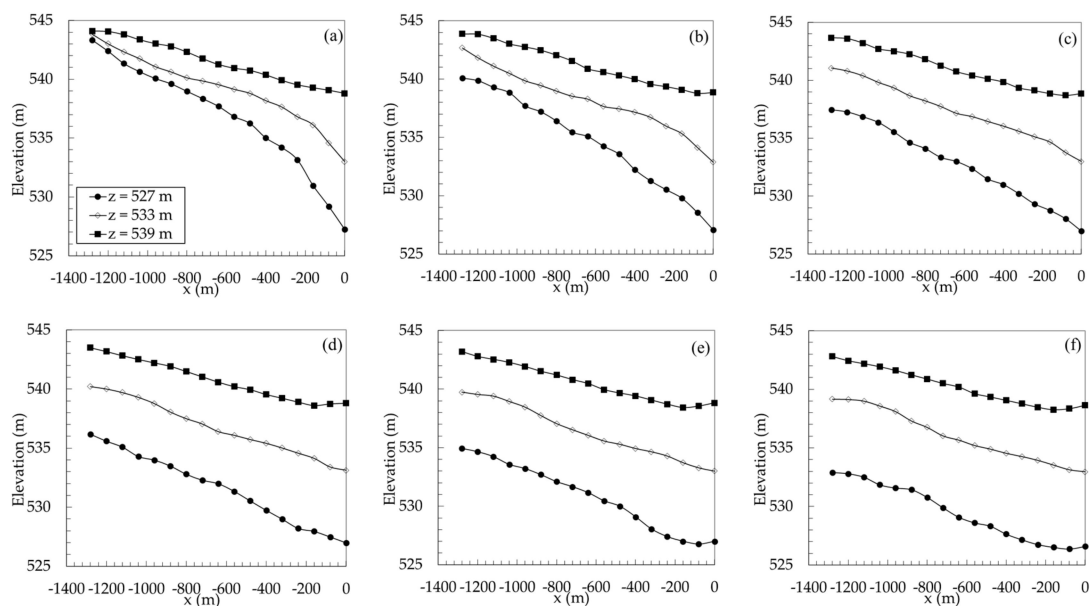

Figure 5. Upstream talweg profile of each GCDs z for $P = 50\%$ (**a**), $P = 20\%$ (**b**), $P = 10\%$ (**c**), $P = 5\%$ (**d**), $P = 3.3\%$ (**e**) and $P = 1\%$ (**f**).

Figure 6 highlights the dependence of the average upstream bed gradient i on the flood discharge Q. Figure 6 shows that i is greater with a lower z. As the GCD drop enlarges the elevation difference between $x = 1300$ m and $x = 0$, the bed tends to develop to be steeper. Figure 6 also indicates that i is approximately independent of Q for $z = 539$ m, but decreases with Q for $z = 533$ m and $z = 527$ m. As shown in Figures 4 and 5, the final bed elevation at $x = 0$ is fixed at the GCD. Thus, the increasing Q erodes more sediment from the upstream bed, resulting in a lower upstream bed level and a smaller average gradient.
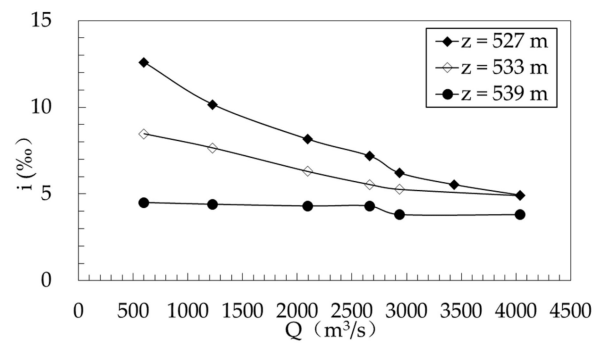
Figure 6. Dependence of average talweg gradient i on discharge Q for different GCDs z.

4.2. Transverse Profile Upstream of GCS

Figure 7 indicates that, for each z, the channel cross-section is deeper and wider with a higher Q. This is because the increase in Q increases the sediment transport capacity of the flow, resulting in greater erosion of the riverbed and riverbanks. Figure 7 also shows that, for a lower z, the difference in the cross-section depth and width caused by increasing Q is greater. More specifically, as shown in Figure 8, the channel cross-section of each discharge is wider and deeper for a lower z. The GCD drop can cause significant bed incision as shown in Figures 4 and 5, inducing mass failures in the riverbank as the incised bed can not support the bank material. Our experimental observations also confirm that, for a lower GCD, more mass failure occurs in the bank.
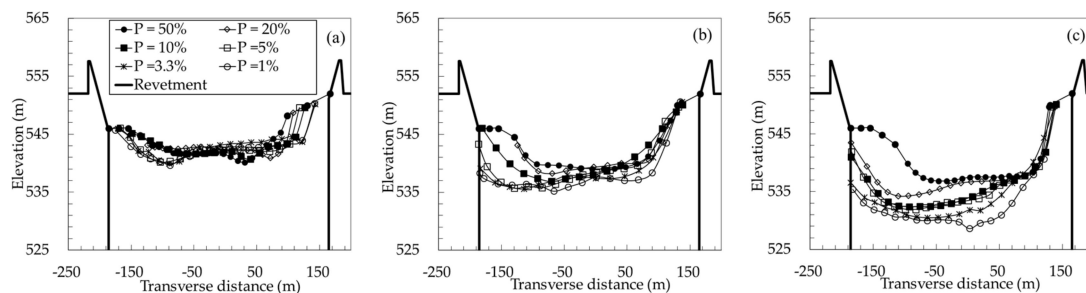

Figure 7. Transverse profile of different flood events (P = 1%–50%) at $x = -800$ m for $z = 539$ m (**a**), $z = 533$ m (**b**) and $z = 527$ m (**c**).
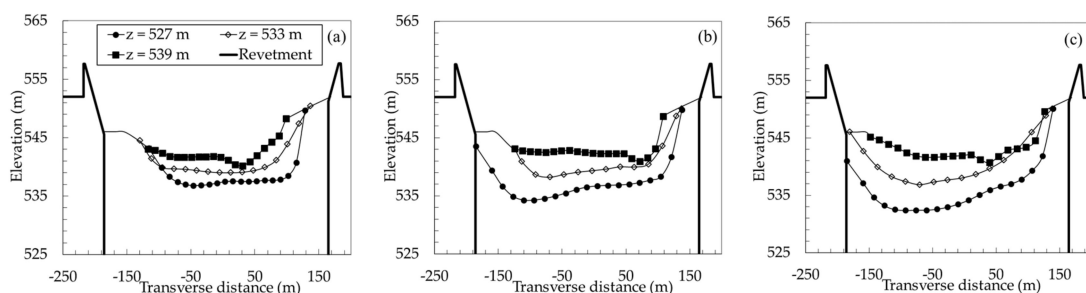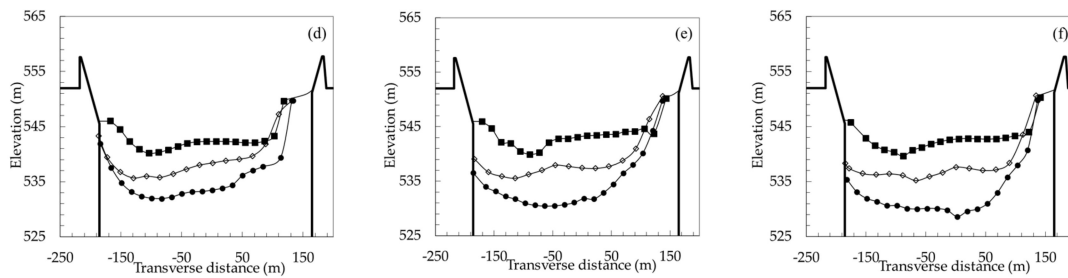

Figure 8. *Cont.*

Figure 8. Transverse profile of different GCDs z for P = 50% (**a**), P = 20% (**b**), P = 10% (**c**), P = 5% (**d**), P = 3.3% (**e**) and P = 1% (**f**).

4.3. General Scour Depth at the 105th Provincial Highway Bridge

Figure 9 highlights the dependence of the maximum general scour depth d_p at the 105th Provincial Highway Bridge on the discharge Q for different GCDs. In Figure 9, for z = 539 m, with the help of the GCS, d_p is approximately independent of Q. For a lower z, even very small Q (P = 50%) can cause serious general scour at the bridge site ($d_p \approx$ 9.4 m and 14.8 m). For z = 527 m, i.e., the GCS is completely removed, the d_p can reach up to 17.6 m. For the new GCS design plan z = 533 m, the minimum d_p is 9.4 m. Thus, this study suggests building a new GCS with $z \geq$ 539 m or a new bridge with much deeper foundations.
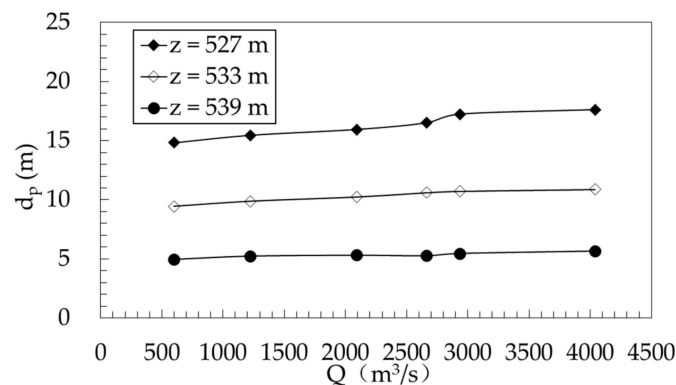

Figure 9. Dependence of the maximum general scour depth d_p at the 105th Provincial Highway Bridge on discharge Q for different GCDs z.

5. Conclusions

Bed degradation is a common river process and can cause general scour depth at instream infrastructures, leading to structural damages or failures. Grade control structures (GCSs) are conventional countermeasures for the general scour at instream structures. However, improper scour design for the GCS can destabilize both the GCS and the upstream river reach. This study conducts a 1:80 scaled model test based on a 1.3 km-long reach of Shiting River, China, investigating the effects of GCS failure (drop in GCD) on the upstream river bed morphology.

The experimental results indicate that, for each GCD z, the upstream river bed elevation decreases with increasing discharge Q. For a lower z, the difference caused by increasing Q is greater. For z = 533 m and z = 527 m, a head cut erosion area exists upstream of the GCS for $P \geq$ 20%. For $P \leq$ 10%, the head cut erosion area of z = 533 m and z = 527 m vanishes. The average upstream bed gradient i is approximately independent of Q for z = 539 m; i decreases with increasing Q for z = 533 m and z = 527 m. The experimental results also indicate that, for each z, the increase in Q can widen and deepen the channel. The difference in the channel width and depth caused by increasing Q is greater for a lower z. For each Q, the decrease in z induces a wider and deeper channel.

The maximum general scour depths d_p at the 105th Provincial Highway Bridge are analyzed. For z = 539 m, d_p is approximately independent of Q. For a lower z, d_p increases slightly with increasing

Q. For the new GCS design plan (z = 533 m), the general scour depth at the bridge site is still significant (d_p = 9.4–10.9 m). Thus, this study suggests building a GCS with $z \geq 539$ m or a new bridge with much deeper foundations.

References

1. Yang, Y.; Melville, B.W.; Sheppard, D.M.; Shamseldin, A.Y. Live-Bed Scour at Wide and Long-Skewed Bridge Piers in Comparatively Shallow Water. *J. Hydraul. Eng.* **2019**, *145*, 06019005. [CrossRef]
2. Yang, Y.; Melville, B.W.; Sheppard, D.M.; Shamseldin, A.Y. Clear-Water Local Scour at Skewed Complex Bridge Piers. *J. Hydraul. Eng.* **2018**, *144*, 04018019. [CrossRef]
3. Guan, D.; Chiew, Y.-M.; Melville, B.W.; Zheng, J. Current-induced scour at monopile foundations subjected to lateral vibrations. *Coast. Eng.* **2019**, *144*, 15–21. [CrossRef]
4. Guan, D.; Chiew, Y.-M.; Wei, M.; Hsieh, S.-C. Characterization of horseshoe vortex in a developing scour hole at a cylindrical bridge pier. *Int. J. Sediment Res.* **2019**, *34*, 118–124. [CrossRef]
5. Guan, D.; Hsieh, S.-C.; Chiew, Y.-M.; Low, Y.M. Experimental study of scour around a forced vibrating pipeline in quiescent water. *Coast. Eng.* **2019**, *143*, 1–11. [CrossRef]
6. Chiew, Y.M. Mechanics of Local Scour Around Submarine Pipelines. *J. Hydraul. Eng.* **1990**, *116*, 515–529. [CrossRef]
7. Wu, Y.; Chiew, Y.-M. Mechanics of Pipeline Scour Propagation in the Spanwise Direction. *J. Waterw. Port Coast. Ocean Eng.* **2015**, *141*, 04014045. [CrossRef]
8. Guan, D.; Melville, B.W.; Friedrich, H. Local scour at submerged weirs in sand-bed channels. *J. Hydraul. Res.* **2016**, *54*, 172–184. [CrossRef]
9. Wang, L.; Melville, B.W.; Whittaker, C.N.; Guan, D. Scour estimation downstream of submerged weirs. *J. Hydraul. Eng.* **2019**. [CrossRef]
10. Wang, L.; Melville, B.W.; Guan, D. Effects of Upstream Weir Slope on Local Scour at Submerged Weirs. *J. Hydraul. Eng.* **2018**, *144*, 04018002. [CrossRef]
11. Wang, L.; Melville, B.W.; Guan, D.; Whittaker, C.N. Local Scour at Downstream Sloped Submerged Weirs. *J. Hydraul. Eng.* **2018**, *144*, 04018044. [CrossRef]
12. Guan, D.; Melville, B.W.; Friedrich, H. Live-Bed Scour at Submerged Weirs. *J. Hydraul. Eng.* **2015**, *141*, 04014071. [CrossRef]
13. Breusers, H.; Raudkivi, A.J. *Scouring*; A.A. Balkema: Rotterdam, The Netherlands, 1991.
14. Hoffmans, G.J.; Verheij, H.J. *Scour Manual*; CRC Press: Boca Raton, FL, USA, 1997; Volume 96.
15. Melville, B.W.; Coleman, S.E. *Bridge Scour*; Water Resources Publication: Highlands Ranch, CO, USA, 2000.
16. Radspinner, R.; Diplas, P.; Lightbody, A.; Sotiropoulos, F. River Training and Ecological Enhancement Potential Using In-Stream Structures. *J. Hydraul. Eng.* **2010**, *136*, 967–980. [CrossRef]
17. Martín-Vide, J.P.; Andreatta, A. Disturbance Caused by Bed Sills on the Slopes of Steep Streams. *J. Hydraul. Eng.* **2006**, *132*, 1186–1194. [CrossRef]
18. Martín-Vide, J.P.; Andreatta, A. Channel degradation and slope adjustment in steep streams controlled through bed sills. *Earth Surf. Process. Landf.* **2009**, *34*, 38–47. [CrossRef]
19. Wang, L.; Melville, B.W.; Whittaker, C.N.; Guan, D. Effects of a downstream submerged weir on local scour at bridge piers. *J. Hydro Environ. Res.* **2018**, *20*, 101–109. [CrossRef]
20. Jeon, J.; Lee, J.Y.; Kang, S. Experimental Investigation of Three-Dimensional Flow Structure and Turbulent Flow Mechanisms Around a Nonsubmerged Spur Dike with a Low Length-to-Depth Ratio. *Water Resour. Res.* **2018**, *54*, 3530–3556. [CrossRef]

21. Ben Meftah, M.; Mossa, M. Scour holes downstream of bed sills in low-gradient channels. *J. Hydraul. Res.* **2006**, *44*, 497–509. [CrossRef]

22. Pagliara, S.; Kurdistani, S.M. Scour downstream of cross-vane structures. *J. Hydro Environ. Res.* **2013**, *7*, 236–242. [CrossRef]

23. Pagliara, S.; Mahmoudi Kurdistani, S. Clear water scour at J-Hook Vanes in channel bends for stream restorations. *Ecol. Eng.* **2015**, *83*, 386–393. [CrossRef]

24. Tregnaghi, M.; Marion, A.; Bottacin-Busolin, A.; Tait, S.J. Modelling time varying scouring at bed sills. *Earth Surf. Process. Landf.* **2011**, *36*, 1761–1769. [CrossRef]

25. Tregnaghi, M.; Marion, A.; Coleman, S. Scouring at Bed Sills as a Response to Flash Floods. *J. Hydraul. Eng.* **2009**, *135*, 466–475. [CrossRef]

26. Tregnaghi, M.; Marion, A.; Coleman, S.; Tait, S. Effect of Flood Recession on Scouring at Bed Sills. *J. Hydraul. Eng.* **2010**, *136*, 204–213. [CrossRef]

27. Tregnaghi, M.; Marion, A.; Gaudio, R. Affinity and similarity of local scour holes at bed sills. *Water Resour. Res.* **2007**, *43*. [CrossRef]

28. Bormann, N.E.; Julien, P.Y. Scour Downstream of Grade-Control Structures. *J. Hydraul. Eng.* **1991**, *117*, 579–594. [CrossRef]

29. D'Agostino, V.; Ferro, V. Scour on Alluvial Bed Downstream of Grade-Control Structures. *J. Hydraul. Eng.* **2004**, *130*, 24–37. [CrossRef]

30. Lenzi, M.A.; Marion, A.; Comiti, F. Local scouring at grade-control structures in alluvial mountain rivers. *Water Resour. Res.* **2003**, *39*, 1176. [CrossRef]

31. Scurlock, S.M.; Thornton, C.I.; Abt, S.R. Equilibrium Scour Downstream of Three-Dimensional Grade-Control Structures. *J. Hydraul. Eng.* **2011**, *138*, 167–176. [CrossRef]

32. Lenzi, M.A.; Marion, A.; Comiti, F.; Gaudio, R. Local scouring in low and high gradient streams at bed sills. *J. Hydraul. Res.* **2002**, *40*, 731–739. [CrossRef]

33. Gaudio, R.; Marion, A.; Bovolin, V. Morphological effects of bed sills in degrading rivers. *J. Hydraul. Res.* **2000**, *38*, 89–96. [CrossRef]

34. Marion, A.; Tregnaghi, M.; Tait, S. Sediment supply and local scouring at bed sills in high-gradient streams. *Water Resour. Res.* **2006**, *42*, W06416. [CrossRef]

35. Marion, A.; Lenzi, M.A.; Comiti, F. Effect of sill spacing and sediment size grading on scouring at grade-control structures. *Earth Surf. Process. Landf.* **2004**, *29*, 983–993. [CrossRef]

36. Lenzi, M.A.; Marion, A.; Comiti, F. Interference processes on scouring at bed sills. *Earth Surf. Process. Landf.* **2003**, *28*, 99–110. [CrossRef]

37. Lu, J.-Y.; Hong, J.-H.; Chang, K.-P.; Lu, T.-F. Evolution of scouring process downstream of grade-control structures under steady and unsteady flows. *Hydrol. Process.* **2012**, *27*, 2699–2709. [CrossRef]

38. Guan, D.; Melville, B.W.; Friedrich, H. Flow Patterns and Turbulence Structures in a Scour Hole Downstream of a Submerged Weir. *J. Hydraul. Eng.* **2014**, *140*, 68–76. [CrossRef]

39. Fan, N.; Nie, R.; Wang, Q.; Liu, X. Dramatic undercutting of piedmont rivers after the 2008 Wenchuan Ms 8.0 Earthquake. *Sci. Rep.* **2016**, *6*, 37108. [CrossRef]

40. Nie, R.; Wang, X.; Liu, F.; Wang, Q.; Fan, N.; Liu, X. Study on Fluvial Processes of Piedmont Rivers Damaged by Strong Earthquakes. *Adv. Eng. Sci.* **2018**, *50*, 105–111. [CrossRef]

41. ASCE. *Hydraulic Modeling: Concepts and Practices*; ASCE: Reston, VA, USA, 2000. [CrossRef]

42. Chien, N.; Wan, Z. *Mechanics of Sediment Transport*; ASCE Press: Reston, VA, USA, 1999. [CrossRef]